Proceedings of ASME 2006
ASME 2006 International Mechanical Engineering Congress and Exposition, Winter Annual Meeting of the ASME
November 5–10, 2006, Chicago, IL, USA

IMECE2006-15296

ACCURATE INTERPRETATION OF MAGNETIC SHAPE MEMORY ALLOY EXPERIMENTS UTILIZING COUPLED MAGNETOSTATIC ANALYSIS

Dimitris C. Lagoudas*
Department of Aerospace Engineering
Texas A&M University
College Station, Texas 77843-3141
Email: lagoudas@aero.tamu.edu

Bjoern Kiefer
Alica J. Broederdorf
Department of Aerospace Engineering
Texas A&M University
College Station, Texas 77843-3141

ABSTRACT

In order to build a reliable constitutive model for magnetic shape memory alloys (MSMAs) the availability of accurate experimental data for calibration and validation purposes is essential. However, the demagnetization effect and the resulting sample shape-dependent difference between the applied field and the internal field makes measurements of MSMAs properties difficult to interpret. Since for non-ellipsoidal specimen the internal magnetic field and thus the induced magnetization is nonuniform, standard demagnetization factors can not be applied without evaluation of the expected error. Following up on previous work by the authors this paper describes a methodology by which experimental data can be interpreted more accurately. The procedure involves the numerical solving of nonlinear magnetostatic boundary value problems for MSMAs in which the stress-dependent magnetic properties of the material are predicted by the constitutive model. New results of this analysis presented here include a parametric study of the sample shape dependence of the demagnetization effect when accounting for the nonlinear magnetization properties of MSMAs.

INTRODUCTION

Magnetic shape memory alloys have recently drawn considerable research interest [1–7] due to their ability to produce magnetic field-induced strains (MFIS) at least one order of magnitude higher than those of ordinary magnetostrictive materials. These inelastic strains are comparable to the temperature- or stress-induced transformation strains in conventional shape memory alloys (SMAs), but are obtainable at frequencies of up to 1 kHz. The observed nonlinear, hysteretic and stress-dependent strain response is caused by the rearrangement of martensitic variants driven by applied magnetic fields. The shape change is coupled to a nonlinear change of the magnetization. As in regular ferromagnetic materials, the magnetization in MSMA also changes through the mechanisms of magnetic domain wall motion and the local rotation of magnetization vectors.

While previous work by the authors has mainly concentrated on the formulation of a continuum level constitutive model for MSMAs [8–11], is has become evident that the model development can not progress without accurate experimental data for model validation purposes. However, measured strain and magnetization data always depend on the specimen geometry and need to be corrected for the demagnetization effect. Since the induced magnetization in the sample is nonuniform, standard techniques involving demagnetization factors can only lead to approximate corrections. Shield [6] commented on this problem, which was also addressed in recent work by the authors [12]. This paper describes a methodology in which the solution of magnetostatic boundary value problems for the MSMA sample provides the shape-dependent relation between the applied field and the internal magnetic field that is needed to properly interpret the experimental data. Since most often only the magnetic field-

*Address all correspondence to this author.

induced strain can be measured in experiments, but not the induced magnetization response, the constitutive model is utilized to determine the magnetization response of the MSMA sample, which is then used as input to the magnetostatic problem.

The structure of the paper is as follows: first, the general magnetomechanical boundary value problem is defined in the following section. The constitutive model is summarized in the subsequent section. Then, specific magnetostatic boundary values problem are solved for prismatic specimen of different aspect ratios and the results are analyzed in detail.

THE MAGNETOMECHANICAL BOUNDARY VALUE PROBLEM

In the following paragraphs basic concepts of magnetostatics in the presence of magnetized matter are summarized to provide the foundation for the analysis of magnetostatic boundary value problems (BVPs) for MSMA materials. For static conditions in stationary bodies and negligible free currents, Maxwell's equations in $\mathbb{R}^3$, the space occupied by the magnetized body and the infinite surrounding free space, reduce to [13, 14]

$$\nabla\cdot\mathbf{B}=0\,,\quad \text{and}\quad \nabla\times\mathbf{H}=0\,,\quad \text{in }\mathbb{R}^3\,, \tag{1}$$

where $\mathbf{B}$ is the magnetic flux density and $\mathbf{H}$ is the magnetic field strength. These two quantities are related through the constitutive relation $\mathbf{B}=\mu_0(\mathbf{H}+\mathbf{M})$, in which μ_0 is the permeability of free space and $\mathbf{M}$ is the magnetization. The magnetization is defined at all material points within the magnetized body, in this case the magnetic shape memory alloy sample. The field variables that result from the solution of Eqns. (1) are subject to the jump conditions

$$[\![\mathbf{B}]\!]\cdot\mathbf{n}=0\,,\quad [\![\mathbf{H}]\!]\times\mathbf{n}=0\,, \tag{2}$$

on all interfaces, where surface currents have again been considered negligible. The jump of a generic field A is defined as $[\![A]\!]=A^+-A^-$. The sign superscript refers to the direction of the unit normal $\mathbf{n}$. As a consequence the normal component of the flux density and the tangential component of the field strength have to be continuous over any interface.

Taking advantage of the specific form of Eqns. (1), the magnetostatic problem is often reformulated by deriving the magnetic field strength from a scalar potential or the flux density from a vector potential. In the latter case $\mathbf{B}=\nabla\times\mathbf{A}$ identically satisfies the first Gauss' law, which is the first equation in (1). Using the identity $\nabla\times(\nabla\times\mathbf{A})=\nabla(\nabla\cdot\mathbf{A})-\Delta\mathbf{A}$, and the Coulomb gauge $\nabla\cdot\mathbf{A}=0$ [13], the second equation in (1), known as Ampère's law, takes the form

$$\nabla\times(\mu_0^{-1}\nabla\times\mathbf{A}-\mathbf{M})=0\,,\quad \text{or}\quad \Delta\mathbf{A}=-\mu_0\nabla\times\mathbf{M}\quad \text{in }\mathbb{R}^3\,, \tag{3}$$

which is the vector-valued Poisson equation for the magnetic potential $\mathbf{A}$. Δ denotes the vector-valued Laplace operator.

As a consequence of the Eqns. (1) and (2), a magnetic body is subjected to the magnetostatic field caused by its own magnetization in such a manner that it tends to demagnetize it. This *demagnetization effect* has relevance when measuring the magnetization response of magnetic materials, since the resulting difference between the externally applied field and internal magnetic field makes experimental data difficult to interpret. Generic integral representations of the magnetic field as resulting from Eqns. (1) exist [13, 15]. For uniformly magnetized bodies the magnetization vector can be taken outside the integral, which then takes the form

$$\mathbf{H}(\mathbf{r})=-\left[\frac{1}{4\pi}\iint_{\partial\Omega}\frac{\mathbf{r}-\mathbf{r}'}{|\mathbf{r}-\mathbf{r}'|^3}\otimes\mathbf{n}'\,\mathrm{d}A'\right]\mathbf{M}=-\mathbf{D}\mathbf{M}\,, \tag{4}$$

where $\mathbf{r}$ is the position at which $\mathbf{H}$ is evaluated in $\mathbb{R}^3$ and $\mathbf{r}'$ the location of a point on the surface $\partial\Omega$, with unit outward normal $\mathbf{n}'$, of the region Ω occupied by the magnetized body. By applying the divergence theorem an equivalent volume integral representation of Eqn. (4) can be obtained. The magnetic field caused by a magnetized body of known uniform magnetization can thus be computed by simply multiplying the magnetization vector with the demagnetization tensor $\mathbf{D}$, which only depends on the geometry of the body and can be computed by evaluating the bracketed integral expression in Eqn. (4). The demagnetization tensor has the following properties: i) it is independent of position inside an ellipsoidal body; ii) it is diagonal if its eigenvectors are aligned with the symmetry axes of the body; iii) its trace is 1, if evaluated inside the body. It has been computed and tabularized for a number of standard geometries and numerical solution schemes have been provided for non-ellipsoidal shapes [16–20].

For uniformly magnetized samples of arbitrary shape average demagnetization factors are defined. If additionally an external field $\mathbf{H}^{\text{applied}}$ is applied, superposition leads to the following expression for the average magnetic field inside a non-ellipsoidal body with uniform magnetization

$$\langle\mathbf{H}\rangle=\mathbf{H}^{\text{applied}}-\langle\mathbf{D}\rangle\mathbf{M}\,. \tag{5}$$

By definition the demagnetization factor loses its meaning for bodies with nonuniform magnetization. In Eqn. (5) the uniformity of $\mathbf{M}$ was simply assumed. However, the magnetization

induced in a non-ellipsoidal body by an external field is always nonuniform unless magnetic saturation is reached everywhere in the body at high fields. Furthermore, if the magnetization is a function of the applied field the magnetostatic problem as described by Eqn. (3) becomes nonlinear and superposition no longer holds Thus for the nonlinear problem involving a magnetized sample of non-ellipsoidal shape whose magnetization is a function of the magnetic field, an explicit numerical solution of the magnetostatic boundary value problem has to be obtained. For MSMAs the problem is complicated by the fact that the magnetic properties are nonlinear, hysteretic and stress-level dependent and that the shape of the sample changes due to the magnetic field-induced strain. The latter aspect, however, is expected to have negligible influence.

In addition to the magnetostatic equations, the boundary value problem is governed by the mechanical equations, namely the conservation of linear and angular momentum for the magnetic continuum [21, 22]

$$\nabla\cdot\boldsymbol{\sigma}+\rho\mathbf{f}+\rho\mathbf{f}^{\mathrm{m}}=0 \qquad \text{in}\,\Omega\,, \tag{6a}$$

$$\operatorname{skw}\boldsymbol{\sigma}=\rho\mathbf{L}^{\mathrm{m}} \quad \text{in}\,\Omega\,, \tag{6b}$$

where ρ is the mass density, $\boldsymbol{\sigma}$ the Cauchy stress tensor and $\mathbf{f}$ the body force. The additional body force $\mathbf{f}^{\mathrm{m}}$ and the body couple $\mathbf{L}^{\mathrm{m}}$ are due to the magnetization of the body and with the assumption of static fields acting on electrically nonpolarized stationary magnetic materials they are given by [22]

$$\rho\mathbf{f}^{\mathrm{m}}=\mu_0(\nabla\mathbf{H})\mathbf{M}\,, \quad \text{and} \quad \rho\mathbf{L}^{\mathrm{m}}=\operatorname{skw}(\mu_0\mathbf{M}\otimes\mathbf{H})\,. \tag{7}$$

By defining the Maxwell stress tensor as [14, 22]

$$\boldsymbol{\sigma}^{\mathrm{M}}=\mu_0\mathbf{H}\otimes\mathbf{H}+\ \mu_0\mathbf{H}\otimes\mathbf{M}-\frac{1}{2}\mu_0(\mathbf{H}\cdot\mathbf{H})\mathbf{I}\,, \tag{8}$$

the equilibrium equations (6) can be rewritten as

$$\nabla\cdot\left(\boldsymbol{\sigma}+\boldsymbol{\sigma}^{\mathrm{M}}\right)+\rho\mathbf{f}=0 \quad \text{in}\,\Omega\,, \tag{9a}$$

$$\operatorname{skw}\left(\boldsymbol{\sigma}+\boldsymbol{\sigma}^{\mathrm{M}}\right)=0 \quad \text{in}\,\Omega\,, \tag{9b}$$

The following jump conditions apply at all interfaces

$$\left[\!\left[\boldsymbol{\sigma}+\boldsymbol{\sigma}^{\mathrm{M}}\right]\!\right]\cdot\mathbf{n} \quad \text{on}\,\partial\Omega\,. \tag{10}$$

In summary, the coupling between the mechanical and the magnetostatic problem has several contributions:

1. Constitutive relations: The magnetization in Eqn. (3), for example, is not only a function of the magnetic field, but also the applied stress and the loading history through a set of internal state variables ζ. The relation $\mathbf{M}=\mathbf{M}(\boldsymbol{\sigma},\mathbf{H},\zeta)$ is provided by the constitutive model to be introduced shortly.
2. Body forces and body couples (7), captured through Maxwell's stress tensor (8), introduce magnetic field dependence into the equilibrium equations (9);
3. Coupled boundary conditions (10);
4. Deformations of the body, resulting in changes in the domain Ω, affect the solution of the magnetostatic problem (3).

The remaining equations to complete the formulation of the magnetomechanical boundary value problem for MSMAs are the constitutive relations, which are specified in the following section.

THE MSMA CONSTITUTIVE MODEL

A phenomenological model has been proposed by the authors to describe the stress- and magnetic field-induced reorientation of martensitic variants in MSMAs. Since the focus of this paper is on the application of the model in combination with the magnetostatic analysis, only a brief summary shall be given here and the reader is referred to previous publications for more detail [9, 10, 23]. The model is based on the Gibbs free energy function G, in which the Cauchy stress tensor $\boldsymbol{\sigma}$ and the magnetic field strength $\mathbf{H}$ are the independent state variables. The loading history dependence of the constitutive behavior, caused by dissipative effects, is introduced through the evolution of internal state variables. The chosen internal state variables are the variant volume fraction ξ, the magnetic domain volume fraction α and the magnetization rotation angles θ_i. These variables are motivated by experimentally observed changes in the crystallographic and magnetic microstructure [24].

The specific form of the Gibbs free energy for the Kiefer and Lagoudas model [9] is given by

$$\begin{aligned} G&=\hat{G}(\boldsymbol{\sigma},\mathbf{H},\xi,\alpha,\theta_i)\\ &=-\frac{1}{2\rho}\boldsymbol{\sigma}:\mathcal{S}(\xi)\boldsymbol{\sigma}-\frac{\mu_0}{\rho}\mathbf{M}(\xi,\alpha,\theta_i)\cdot\mathbf{H}\\ &\quad+G^{\mathrm{an}}(\xi,\alpha,\theta_i)+G^{\mathrm{mix}}(\xi)+G_0\,, \end{aligned} \tag{11}$$

where $\mathcal{S}$, $\mathbf{M}^{\mathrm{eff}}$ and G^{an} are the effective compliance tensor and magnetocrystalline anisotropy, respectively. The free energy function (11) is comprised of the elastic strain energy, the Zeeman energy, the magnetocrystalline anisotropy energy, a mixing term and a reference state value. The Zeeman or external field energy aims to align the internal magnetization with the externally applied magnetic field. The magnetocrystalline anisotropy

energy can be viewed as the energy stored in the material due to the work done by rotating the magnetization away from the magnetic easy axes. The mixing term accounts for the deviation of the total free energy from the assumed weighted average of the individual variants and magnetic domains due to interactions.

Different combinations of these energy terms have also been included in other constitutive models [3, 25, 26]. Unlike most of these formulations, however, this work is concerned with the influence of dissipative effects on the evolution of thermodynamic states, rather than the minimization of the free energy. This approach has successfully been used in the modeling of conventional shape memory alloys [27, 28].

From the free energy expression (11) the constitutive equations are derived in a thermodynamically-consistent manner [9], such that

$$\varepsilon^{\mathrm{e}} = \varepsilon - \varepsilon^{\mathrm{r}} = -\rho \frac{\partial \hat{G}}{\partial \sigma} , \qquad \text{and} \qquad \mathbf{M} = -\frac{\rho}{\mu_0} \frac{\partial \hat{G}}{\partial \mathbf{H}} , \qquad (12)$$

where an additive decomposition of the total strain into an elastic strain and a reorientation strain has been assumed, and the total infinitesimal strain is related to the displacement field by $\varepsilon = \frac{1}{2}(\nabla \mathbf{u} - (\nabla \mathbf{u})^{\mathrm{T}})$. A reduced form of the remaining constitutive equations is presented in Tab. 1. This simplified set of equations holds for a typical loading case in which only the components σ_{xx} and H_y are non-zero. Relations between the model parameters and material constants for example specified in [9].

Based on these constitutive equations exemplary model predictions of the magnetic field-induced strain and the magnetization response for different constant stress levels are depicted in Fig. 1 and 2, respectively. This particular prediction is based on model parameters calibrated from data published by Heczko et al. 2003 [2]. For more details on these predictions the reader is again referred to [9, 10].

Recently the authors have addressed the impact of magnetic domain wall motion at low magnetic fields. As evident from Eqn. (11), the presented MSMA constitutive model already incorporates the magnetic domain volume fraction α as an internal state variable and its relation to the macroscopic magnetization is defined through Eqn. (12). Previously the evolution of magnetic domains had been neglected based on the argument that unfavorable magnetic domains are eliminated as soon as the reorientation process is activated [10, 11, 29]. This argument can actually only be justified for the forward reorientation process, because it usually occurs at relatively high magnetic fields. The reverse reorientation process, however, occurs at low magnetic fields. In various experiments it has been observed that MSMA typically do not produce remnant magnetization [2, 30], although they do exhibit residual strains. If domain wall motion is neglected at moderate to high stresses, with respect to a scale between zero and the blocking stress, the model predicts that the mechanism

Table 1. SUMMARY OF THE REDUCED MODEL EQUATIONS FOR THE SPECIAL CASE OF UNIAXIAL STRESS AND PERPENDICULAR MAGNETIC FIELD.

Magnetic Field-Induced Strain and Magnetization:

$$\varepsilon^{\mathrm{r}}_{xx} = \varepsilon^{\mathrm{r,max}} \xi \; ; \quad \varepsilon^{\mathrm{r}}_{yy} = -\varepsilon^{\mathrm{r}}_{xx}.$$

$$M_x = (1-\xi) M^{\mathrm{sat}} \sqrt{1 - \left(\frac{\mu_0 M^{\mathrm{sat}}}{4\rho K_1} \right)^2 H_y^2} \; ;$$

$$M_y = \xi M^{\mathrm{sat}} + (1-\xi) M^{\mathrm{sat}} \frac{\mu_0 (M^{\mathrm{sat}})^2}{2\rho K_1} H_y \; .$$

Driving Force for Variant Reorientation:

$$\pi^{\xi} = \sigma \Lambda^{\mathrm{r}}_{xx} - \rho \frac{\partial \hat{G}}{\partial \xi} = \sigma \varepsilon^{\mathrm{r,max}} + \mu_0 M^{\mathrm{sat}} H_y - \frac{(\mu_0 M^{\mathrm{sat}})^2}{4\rho K_1} H_y^2 - \frac{\partial f^{\xi}}{\partial \xi}.$$

2.5ex] **Reorientation Function:**

$$\Phi^{\xi}(\sigma, \mathbf{H}, \xi) = \begin{cases} \pi^{\xi} - Y^{\xi,\mathrm{c}} , & \dot{\xi} > 0 \\ -\pi^{\xi} - Y^{\xi,\mathrm{c}} , & \dot{\xi} < 0 \end{cases} .$$

Kuhn-Tucker Loading Conditions:

$$\Phi^{\xi}(\sigma, \mathbf{H}, \xi) \leq 0, \quad \Phi^{\xi} \dot{\xi} = 0 \; .$$

Hardening Function (Derivative):

$$\frac{\partial f^{\xi,\mathrm{c}}}{\partial \xi} = \begin{cases} -A^{\mathrm{c}} \left[\pi - \cos^{-1}(2\xi - 1) \right] + (B^{\mathrm{c}}_1 + B^{\mathrm{c}}_2) , & \dot{\xi} > 0 \\ -C^{\mathrm{c}} \left[\pi - \cos^{-1}(2\xi - 1) \right] + (B^{\mathrm{c}}_1 - B^{\mathrm{c}}_2) , & \dot{\xi} < 0 \end{cases} .$$

of reverse variant reorientation returns the magnetization to low values of remnant magnetization, but not zero, as can be seen in Fig. 2.

At very low stress levels this problem becomes much more apparent since the recovery of the stress-favored variant is usually not induced. In this case the model predicts a remnant magnetization of M^{sat}. If one is interested in an accurate prediction of the magnetization behavior of MSMAs at low magnetic field and low stresses and not just accurate predictions of the strain response this is unacceptable. By deriving evolution equations from thermodynamic constraints, similar to those derived for the magnetization rotation angles [10, 11], the model was successfully modified to account for the motion of magnetic domain walls in this load regime. An example of reorientation strain and magnetization predictions with magnetic domain wall motion are shown in Figs. 3 and 4.

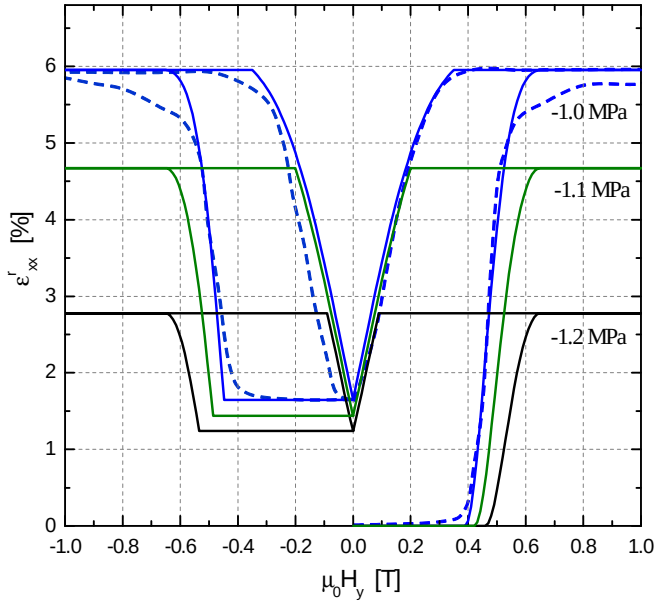

Figure 1. PREDICTED MFIS HYSTERESIS CURVES AT DIFFERENT STRESS LEVELS. SOLID LINES: MODEL, DASHED LINE: EXPERIMENTAL DATA [2].

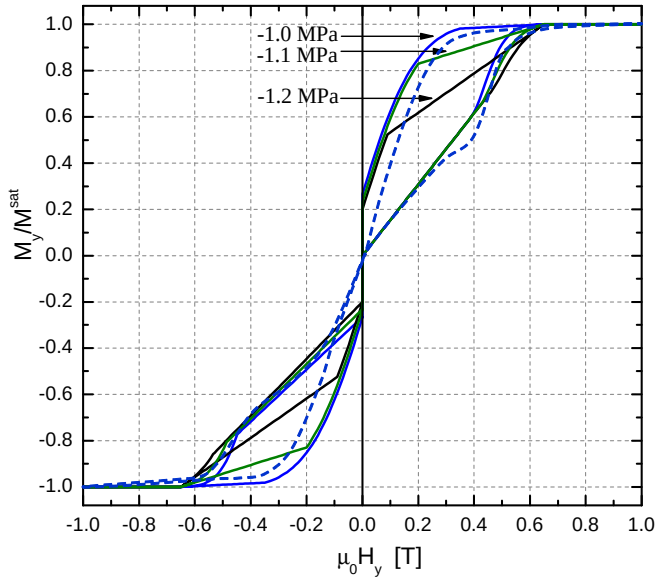

Figure 2. PREDICTED MAGNETIZATION CURVES AT DIFFERENT STRESS LEVELS. SOLID LINES: MODEL, DASHED LINE: EXPERIMENTAL DATA [2].

MAGNETOSTATIC ANALYSIS OF MSMA EXPERIMENTS

Based on the numerical analysis of specific magnetostatic boundary value problems, which have generically been defined

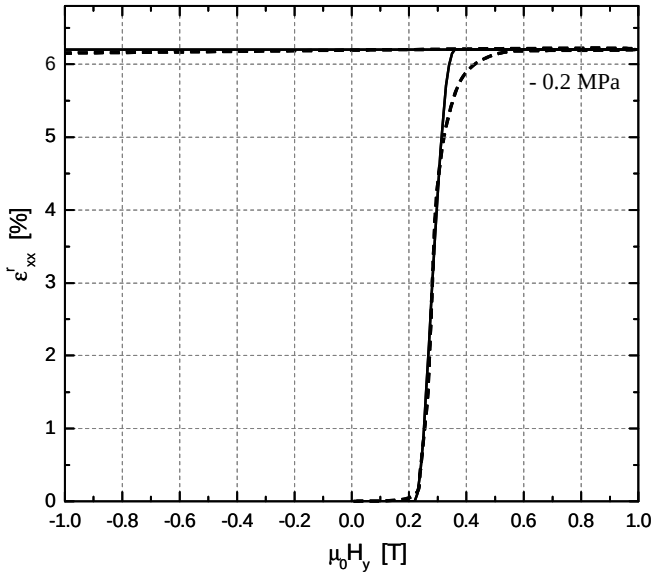

Figure 3. PREDICTED MFIS HYSTERESIS CURVE. SOLID LINES: MODEL, DASHED LINE: EXPERIMENTAL DATA [2].

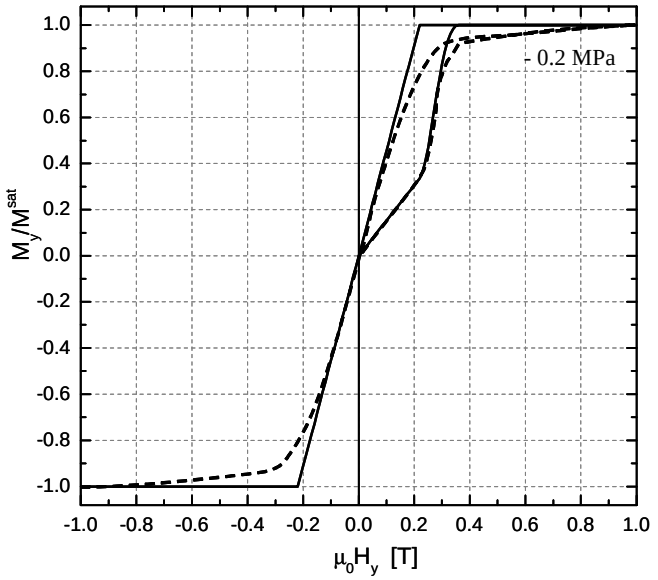

Figure 4. PREDICTED MAGNETIZATION CURVE WHEN ACCOUNTING FOR MAGNETIC DOMAIN WALL MOTION AT LOW MAGNETIC FIELD AND STRESS LEVELS. SOLID LINES: MODEL, DASHED LINE: EXPERIMENTAL DATA [2].

by field equations, constitutive relations and interface jump conditions in the preceding sections, the influence of the demagnetization effect on the interpretability of MSMA experiments is investigated in this section. As described, a typical experiment consists of subjecting a martensitic MSMA sample to a constant

mechanical load and subsequently to a perpendicular magnetic field. This induces the reorientation of the stress-favored variant into the magnetic field-favored variant and is accompanied by the observed large inelastic shape change. The strain response can only be measured as a function of the applied field. However, due to the demagnetization effect the same applied field translates to different internal fields for different geometries. The material, of course, reacts to the internal magnetic field it experiences. To extract the true constitutive response that can be used for model calibration, the data needs therefore needs to be available in terms of the internal magnetic field. The goal of this analysis is to find the relation between the externally applied and the internal magnetic fields for a MSMA sample of specific geometry, which can then be used to properly interpret the experimental data.

A general discussion of the influence of the demagnetization effect on the measuring of magnetization curves in ferromagnetic materials can be found in O'Handley 2002 [16]. Shield [6] addressed the problem for experiments on magnetic shape memory materials by approximating his samples as uniformly magnetized rectangular bars, in which case a constant demagnetization factor according to Eqn. (5) can be utilized. Here, the more general problem of nonuniform magnetization is considered for the following reasons:

1. To take the first step towards solving the fully-coupled boundary value problem;
2. To improve the accuracy with which experimental results can be interpreted. Example: The investigation of the influence of the nonuniformity of the magnetization on the relation between the internal and applied magnetic field;
3. To improve the experiments themselves. Example: The optimal placement of the Hall probe that measures the applied field can be evaluated, if the distribution of the magnetic field around the specimen is known;

The geometry of the boundary value problem to be solved is determined by considering typical sample dimensions of $8\,\mathrm{mm}\times 4\,\mathrm{mm}\times 4\,\mathrm{mm}$, or aspect ratios of $2:1:1$, with respect to the axial load direction x, the applied field direction y and the remaining transverse direction z. Due to the numerical complexity of the problem and for illustration purposes, however, the analysis is performed in two-dimensions, which, with an in-plane aspect ratio of $2:1$, essentially assumes that the specimen extends to infinity in the z-direction. All of the conclusion that will be drawn from this analysis, however, are generalizable to three dimensions. According to electromagnet specification, a uniform magnetic field can be assumed in a gap of the dimensions $26\,\mathrm{mm}\times 26\,\mathrm{mm}\times 26\,\mathrm{mm}$. For the numerical analysis of the magnetostatic problem (3), subject to the jump conditions (2), the finite element mesh depicted in Fig. 5 is used. This figure also indicates the location of the specimen, and the nonmagnetic grips (dashed lines). A constant magnetic flux of $B_y^{\text{applied}} = \mu_0 H_y^{\text{applied}}$ is applied on the boundary.

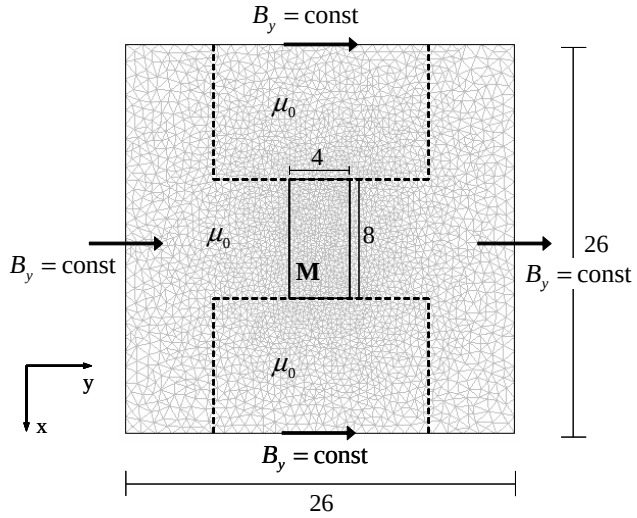

Figure 5. DOMAIN GEOMETRY, MESH AND BOUNDARY CONDITIONS FOR THE MAGNETOSTATIC PROBLEM. DASHED LINES INDICATE THE LOCATION OF THE NONMAGNETIC GRIPS OF THE LOAD FRAME.

All magnetostatic analysis was performed using the COMSOL Multiphysics (FEMLAB) finite element software package. For the purpose of validation specimen of constant magnetization were analyzed and the numerically computed demagnetization factors were compared to literature values [16–20]. For the constant magnetization specimen of aspect ratio $2:1$, average demagnetization factor components (cf. Eqn. (5)) of

$$\begin{aligned} \langle D_{xx}\rangle &= -\langle H_x\rangle / M_x = 0.355\,; \\ \langle D_{yy}\rangle &= -\langle H_y\rangle / M_y = 0.651\,, \end{aligned} \tag{13}$$

were computed.

In order to determine the relation between the applied and the internal magnetic field, without making the assumption of uniformity of the induced magnetization, the following procedure is proposed:

1. Since only a few experimental setups exist in which the MFIS and the magnetization can be measured simultaneously [2, 6], it is assumed that only the MFIS data as a function of the applied magnetic field and stress level is available from experiments. The magnetization curves needed for the analysis are predicted by the constitutive model, cf. Fig. 2, which uses the MFIS data for calibration, in addition to the saturation magnetization and the magnetocrystalline anisotropy constant [23].
2. The magnetization curves $M_x(H_y)$, $M_y(H_y)$ are used as input to the magnetostatic analysis. The coupling between the

mechanical and the magnetic problem in this case exists in the fact that the magnetization curves at different stress levels lead to different solutions of the magnetostatic problem. Magnetic body forces and body couples are neglected, and it is assumed that the changes in geometry due to the magnetic field-induced strains are small enough to be neglected.

3. The problem is solved via finite element analysis. Note that the posed problem is highly nonlinear, since the magnetization on the right hand side of the governing Poisson equation (3) depends on the unknown magnetic potential. With the numerical solution, the relation between internal and applied magnetic fields is established. This relation is used to correct the initially assumed magnetization curves.
4. The magnetostatic problem is solved again with the updated magnetization data as input. This iterative procedure leads to the desired solution of the inverse problem of trying to find the correct internal magnetic field which results in the MFIS vs. applied magnetic field curves measured in the experiment.

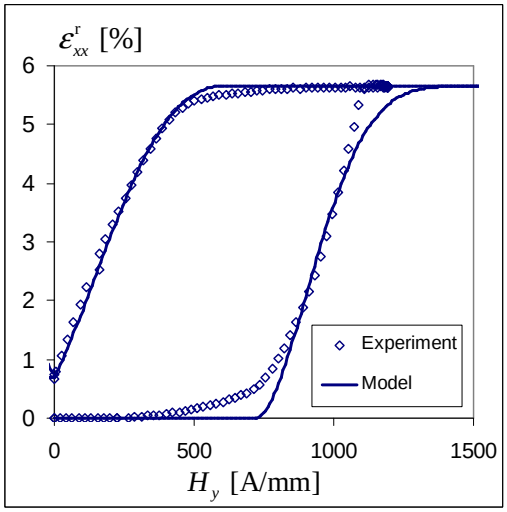

Figure 6. MODEL CALIBRATION. EXPERIMENTAL DATA (DIAMONDS) AND MODEL SIMULATION (SOLID LINE). DATA TAKEN FROM [23] FOR A $Ni_{51.1}Mn_{24.0}Ga_{24.9}$ ALLOY TESTED AT - 95 $^{\circ}C$ UNDER THE COMPRESSIVE STRESS OF 2 MPa.

Following this procedure, Fig. 6 depicts the MFIS data used for calibration[1] and the resulting model simulation for a typical experiment. The corresponding magnetization curves shown in Fig. 7 have been predicted by the constitutive model which has been defined through Eqns. (11) and (12) and the equations of Table 1.

[1]The calibration of model parameters has been described in detail in previous publications. [9, 10]

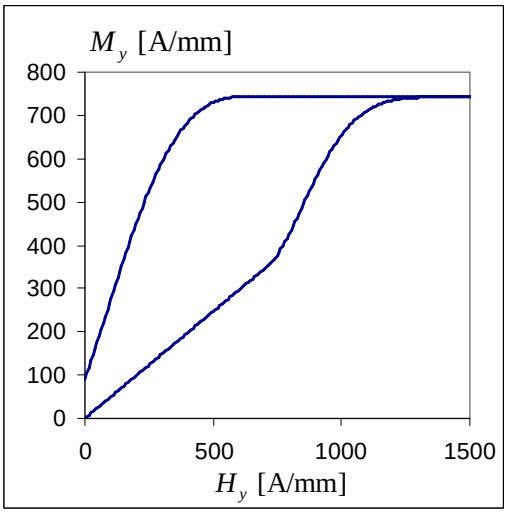

Figure 7. Y-COMPONENT OF THE PREDICTED MAGNETIZATION AT THE COMPRESSIVE STRESS OF 2 MPa.

The following assumptions are made for the use of the magnetization data in the finite element analysis: i) To be consistent with the formulation of the model, the effect of the motion of 180° domain walls is neglected, since these are expected to only occur at low magnetic fields. As a consequence the single crystal specimen is initially magnetized in the axial direction even for zero applied field in the transverse direction. The magnetization in the specimen therefore changes only by its rotation and the reorientation of martensitic variants, which is represented by the nonlinearity of the magnetization curve; ii) Even though the x-component of the applied magnetic field is zero, the same does not hold for the internal field, due to the magnetization of the body and the shape of the specimen (corner effects). However, the influence of the x-component of the internal magnetic field is neglected; iii) The magnetization component $M_x = M_x(H_y)$ is assumed to be dominated by the component $M_y = M_y(H_y)$ and therefore neglected; iv) The hysteretic nature of the constitutive response is not addressed in the magnetostatic analysis at this point. To be precise, the hysteresis is not neglected, but the analysis is only carried out from 0 T to 2.5 T, not for the removal of the magnetic field.

The solution of the finite element analysis of the specified nonlinear magnetostatic problem, with all the described assumptions, is plotted in Fig. 8 in terms of the change in the distribution of H_y as a function of the applied field. It is observed that indeed, due to the non-ellipsoidal shape of the specimen, the magnetic field and thus the magnetization are nonuniform inside the specimen. Fig. 8 also displays the influence of the specimen magnetization on its surroundings, in which the magnetic field without the presence of the specimen would be constant. It is evident from this analysis the Hall probe for measuring the applied field must be placed with care, to minimize the contamination of

its readings. The depicted arrows have been added to illustrate the current orientation of the average specimen magnetization. The magnetization, however, changes locally and the local magnetization is comprised of the contributions of both martensitic variants at the scale of the underlying microstructure, whose volume fractions change with the applied field.

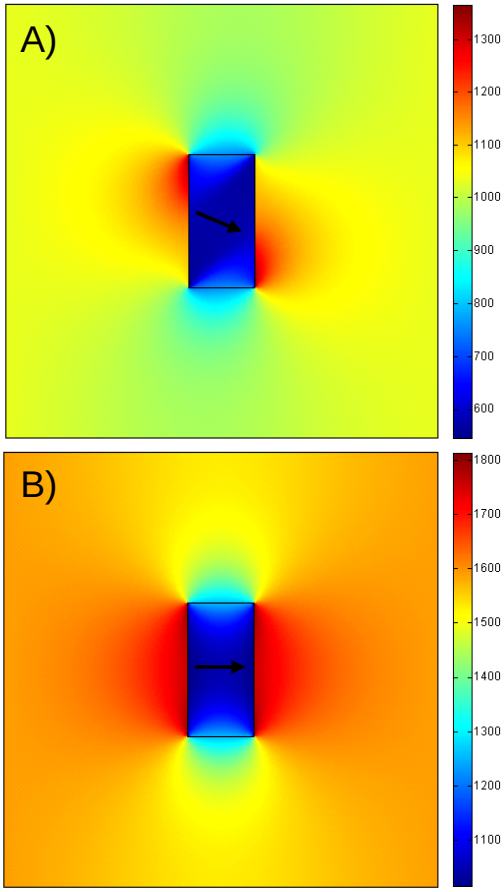

Figure 8. DISTRIBUTION OF H_y IN THE COMPUTATIONAL DOMAIN AN APPLIED MAGNETIC FLUX DENSITY OF A) 1.3 T, B) 2.0 T. (OR IN FIELD STRENGTH: A) 1034.5 A/mm, B) 1591.6 A/mm).

To further investigate the local behavior, the variation of the magnetic field within the MSMA sample is plotted in Fig. 9 for two different applied field levels. The 1.3 T case is particularly interesting because it falls into the region in which variant reorientation occurs (cf. Fig. 7).

INTERPRETATION OF THE RESULTS

After obtaining the solution to the magnetostatic problem, the next step is to use the computed relation between the applied and internal magnetic field to reinterpret the experimental magnetic field-induced strain and magnetization curves. The details of this procedure shall be discussed in this section.

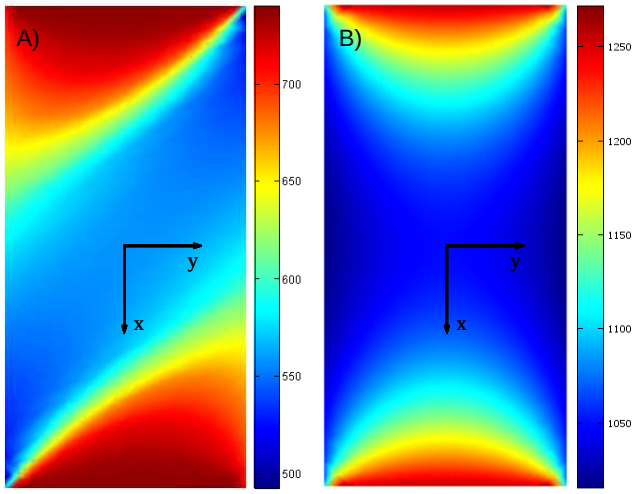

Figure 9. DISTRIBUTION OF H_y WITHIN THE SPECIMEN AT AN APPLIED MAGNETIC FLUX DENSITY OF A) 1.3 T AND B) 2.0 T.

The magnetostatic analysis has been performed in several iterations, each time using the updated data of the last iteration as input for the next. The original and corrected magnetization curves are depicted in Fig. 10 for a specimen with a 2:1 length to width ratio. The corrected curves were plotted by using the same data for the vertical axes, while rescaling the magnetic field axis by means of the relation between the average internal and applied field at each iteration. One observes the relatively fast convergence of the solution. After six iterations the difference to the solution of the previous iteration is almost undetectable. The inverse problem has therefore successfully been solved, meaning the true constitutive behavior of the material has been determined such that if the magnetostatic problem were solved for a material with these magnetic properties and this geometry, one would obtain the original relation $M_y(H_y^{\text{applied}})$.

Fig. 12 compares the different data correction techniques. The standard demagnetization factor method utilizes Eqn. (5) with the $\langle D_{yy} \rangle$ value for this geometry specified in (13). If one assumes that the magnetization is not only spatially homogeneous, but also not a function of the applied field with $M_y = M^{\text{sat}}$, one obtains the correction denoted "D-factor 1". This method is very inaccurate and is only used if data for the magnetization response is not available. If the magnetization response has been measured as a function of the applied field or has been predicted by the constitutive model, as in this case, Eqn. (5) with $M_y = M_y(H_y^{\text{applied}})$, leads to the correction denoted "D-factor 2." It is found that this correction is very close to the correction

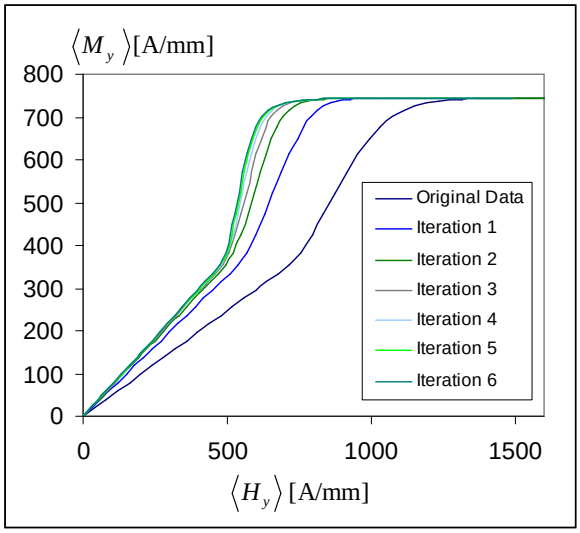

Figure 10. MAGNETIZATION DATA CORRECTED FOR DEMAGNETIZATION. SPECIMEN ASPECT RATIO 2:1.

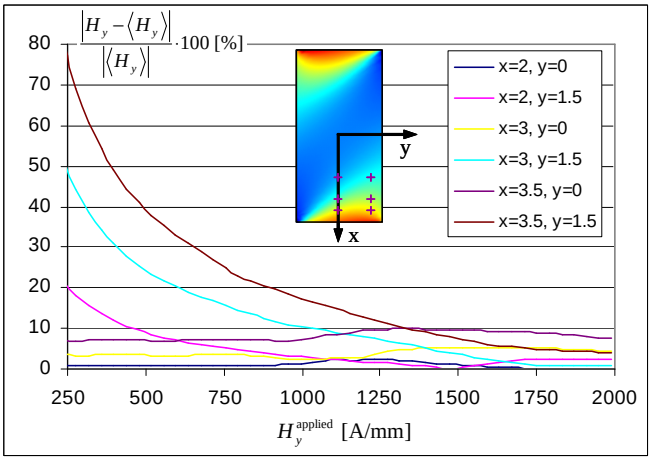

Figure 11. RELATIVE DIFFERENCE IN LOCAL AND AVERAGE H_y AT DIFFERENT LOCATIONS OF THE SPECIMEN VS. APPLIED MAGNETIC FIELD.

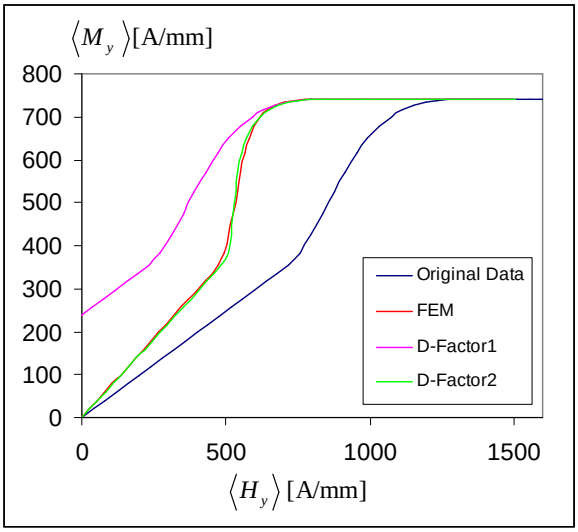

Figure 12. COMPARISON OF THE CORRECTIONS THROUGH DEMAGNETIZATION FACTORS AND FEM ANALYSIS. SPECIMEN ASPECT RATIO 2:1.

obtained from the FEM analysis. These observations suggest that using the demagnetization factor method, which is based on the assumption of uniform magnetization in the specimen, one obtains essentially the same result as performing the FEM analysis of the nonlinear magnetostatic problem with nonuniform magnetization, if average field quantities are considered. This conclusion can be misleading, however, because the difference of local and volume averaged fields can be very large. To emphasize this point the variation of the internal magnetic field as a function of location and applied field is considered. Fig. 11 displays the relative difference of the local field from the volume average at several points in the specimen.[2] For problems in which the knowledge of local magnetic field and magnetization is important, solving the magnetostatic problem explicitly, as performed here, is inevitable. Such cases are certainly encountered if one is interested in solving magnetomechanical MSMA boundary value problems not just involving simple specimen shapes, but for example geometries of active components in actuators.

A parametric study has been performed to evaluate the sample shape dependence of the demagnetization correction. In Fig. 13 the corrected magnetization data has been plotted for four different aspect ratios of the prismatic specimen with square cross-section. The corresponding corrections of the MFIS data have been plotted in Fig. 14. It is clearly observed that the influence of the specimen aspect ratio on the difference between the apparent material behavior and the true constitutive response is very significant and must therefore be addressed when using data for model calibration. Once the MFIS data has been corrected for demagnetization, the model parameters can be recalibrated.[3]

[2]The plots start at 250A/mm, since for small fields the relative differences can be deceivingly large.

[3]The specific results presented here are based on solutions of 2-D boundary value problems and can thus only be used qualitatively. The procedure is the same for 3-D problems, which however are computationally much more involved.

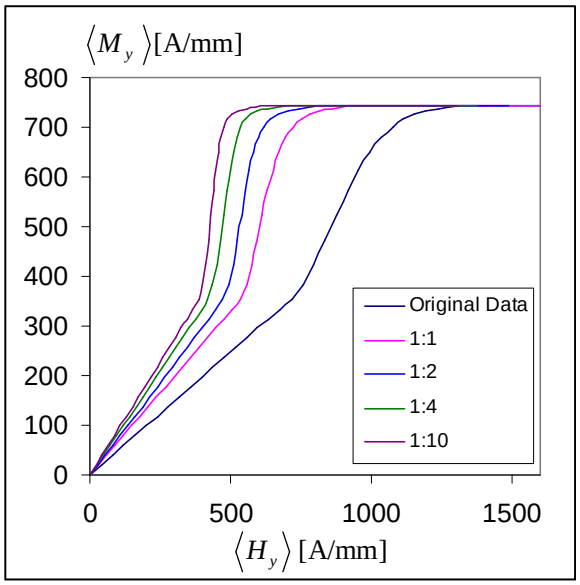

Figure 13. INFLUENCE OF SPECIMEN ASPECT RATIOS ON THE CORRECTION OF THE MAGNETIZATION DATA.

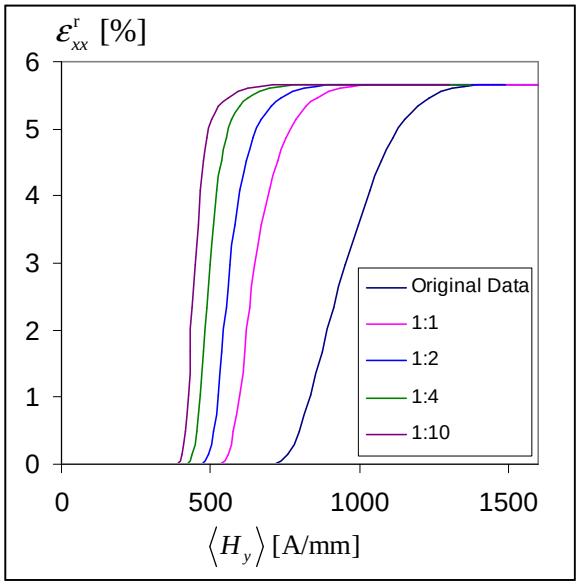

Figure 14. INFLUENCE OF SPECIMEN ASPECT RATIOS ON THE CORRECTION OF THE MFIS DATA.

DISCUSSION

The main results of the work presented in this paper can be summarized as follows:

1. The fully-coupled magnetomechanical boundary value problem involving magnetic shape memory alloy constitutive behavior was formulated.
2. The demagnetization effect in MSMA specimen was investigated by solving magnetostatic boundary value problems in which the only source of mechanical coupling is the stress dependence of the magnetic properties.
3. The nonuniform distribution of the magnetic field inside and around the specimen was determined.
4. The computed relation between the applied and average internal magnetic field was used to correct strain and magnetization curves that were based on experimental data found for a specific specimen shape. For the average fields it was found that demagnetization factors, which assume a uniform induced magnetization in the specimen, lead to a good approximation of the demagnetization effect, if the correct nonlinear magnetization curves are utilized. However, the local fields and the resulting change in the local magnetization deviate vastly from their volume averages.
5. A parametric study of the specimen aspect ratio dependence of the demagnetization effect was presented.

In future work the following issues will be addressed:

1. Solution of the 3-D magnetostatic problem for MSMAs.
2. From the analysis presented in this paper, it is evident that material points inside the specimen will, in general, not exclusively be exposed to the H_y component of the magnetic field, as assumed in the reduction of the constitutive model equations. It is to be investigated whether the other components can reasonably be neglected as is usually done.
3. As the ultimate goal the fully-coupled magnetomechanical boundary value problem for MSMA which was defined in this paper is to be solved.

ACKNOWLEDGMENT

This work was supported by the Army Research Office, contract no. DAAD 19-02-1-0261 and the National Science Foundation, award no. CMS-0324537.

REFERENCES

[1] Yamamoto, T., Taya, M., Sutou, Y., Liang, Y., Wada, T., and Sorensen, L., 2004. "Magnetic field-induced reversible variant rearrangement in Fe-Pd single crystals". *Acta Materialia*, **52**(17), pp. 5083–5091.

[2] Heczko, O., Straka, L., and Ullakko, K., 2003. "Relation between structure, magnetization process and magnetic shape memory effect of various martensites occuring in Ni-Mn-Ga alloys". *Journal de Physique IV France*, **112**, pp. 959–962.

[3] O'Handley, R. C., 1998. "Model for strain and magnetization in magnetic shape-memory alloys". *Journal of Applied Physics*, **83**(6), pp. 3263–3270.

[4] Murray, S. J., Marioni, M., Tello, P. G., Allen, S. M., and O'Handley, R. C., 2001. "Giant magnetic-field-induced strain in Ni-Mn-Ga crystals: Experimental results and modeling". *Journal of Magnetism and Magnetic Materials*, **226–230**(1), pp. 945–947.

[5] Müllner, P., Chernenko, V. A., and Kostorz, G., 2003. "A microscopic approach to the magnetic-field-induced deformation of martensite (magnetoplasticity)". *Journal of Magnetism and Magnetic Materials*, **267**, pp. 325–334.

[6] Shield, T. W., 2003. "Magnetomechanical testing machine for ferromagnetic shape-memory alloys". *Review of Scientific Instruments*, **74**(9), pp. 4077–4088.

[7] Likhachev, A. A., Sozinov, A., and Ullakko, K., 2004. "Different modeling concepts of magnetic shape memory and their comparison with some experimental results obtained in Ni-Mn-Ga". *Material Science & Engineering A*, **378**, pp. 513–518.

[8] Kiefer, B., and Lagoudas, D. C., 2004. "Phenomenological modeling of ferromagnetic shape memory alloys". *Proceedings of SPIE, Smart Structures and Materials: Active Materials: Behavior and Mechanics, San Diego, CA, 14–18 March 2004*, **5387**, pp. 164–176.

[9] Kiefer, B., and Lagoudas, D. C., 2005. "Magnetic field-induced martensitic variant reorientation in magnetic shape memory alloys". *Philosophical Magazine Special Issue: Recent Advances in Theoretical Mechanics, in Honor of SES 2003 A.C. Eringen Medalist G.A. Maugin*, **85**(33-35), pp. 4289–4329.

[10] Kiefer, B., and Lagoudas, D. C., 2005. "Modeling of the magnetic field-induced martensitic variant reorientation and the associated magnetic shape memory effect in MSMAs". *Proceedings of SPIE, Smart Structures and Materials: Active Materials: Behavior and Mechanics, San Diego, CA, 6–10 March 2005*, **5761**, pp. 454–465.

[11] Kiefer, B., and Lagoudas, D. C., 2006. "Modeling of the hysteretic strain and magnetization response in magnetic shape memory alloys". *Proceedings of AIAA 2006*, **paper 1766**, pp. 1–15.

[12] Kiefer, B., and Lagoudas, D., 2006. "Application of a magnetic sma constitutive model in the analysis of magnetomechanical boundary value problems". *Proceedings of SPIE, Smart Structures and Materials: Active Materials: Behavior and Mechanics, San Diego, CA, 26 February–2 March 2006*, **6170**, pp. 330–341.

[13] Jackson, J. D., 1975. *Classical Electrodynamics*, 2nd ed. John Wiley & Sons.

[14] Woodson, H. H., and Melcher, J. R., 1990. *Electromechanical Dynamics, Part I: Discrete Systems*, Reprint of 1968 ed. Krieger Publishing Company.

[15] Bertram, H. N., 1994. *Theory of Magnetic Recording*. Cambridge University Press.

[16] O'Handley, R. C., 2000. *Modern Magnetic Materials*. John Wiley & Sons.

[17] Cullity, B. D., 1972. *Introduction to Magnetic Materials*. Addison-Wesley.

[18] Bozorth, R. M., 1993. *Ferromagnetism*, reissue of 1951 ed. IEEE Press.

[19] Schlömann, E., 1962. "A sum rule concerning the inhomogeneous demagnetizing field in nonellipsoidal samples". *Journal of Applied Physics*, **33**(9), pp. 2825–2826.

[20] Moskowitz, R., and Della Torre, E., 1966. "Theoretical aspects of demagnetization tensors". *IEEE Transactions on Magnetics*, **2**(4), pp. 739–744.

[21] Eringen, A. C., and Maugin, G. A., 1990. *Electrodynamics of Continua I — Foundations and Solid Media*. Springer-Verlag.

[22] Hutter, K., and van de Ven, A. A. F., 1978. *Field Matter Interactions in Thermoelastic Solids*, Vol. 88 of *Lecture Notes in Physics*. Springer-Verlag.

[23] Kiefer, B., Karaca, H. E., Lagoudas, D. C., and Karaman, I., 2006. "Characterization and modeling of the magnetic field-induced strain and work output in Ni_2MnGa shape memory alloys". *Submitted to Journal of Magnetism and Magnetic Materials*.

[24] Sullivan, M. R., and Chopra, H. D., 2004. "Temperature- and field-dependent evolution of micromagnetic structure in ferromagnetic shape-memory-alloys". *Physical Review B*, **70**, pp. 094427–(1–8).

[25] James, R. D., and Hane, K. F., 2000. "Martensitic transformations and shape-memory materials". *Acta Materialia*, **48**(1), pp. 197–222.

[26] Hirsinger, L., and Lexcellent, C., 2003. "Internal variable model for magneto-mechanical behaviour of ferromagnetic shape memory alloys Ni-Mn-Ga". *Journal de Physique IV France*, **112**, pp. 977–980.

[27] Lagoudas, D. C., Bo, Z., and Qidwai, M. A., 1996. "A unified thermodynamic constitutive model for SMA and finite element analysis of active metal matrix composites". *Mechanics of Composite Materials and Structures*, **3**, pp. 153–179.

[28] Boyd, J. G., and Lagoudas, D. C., 1996. "A thermodynamical constitutive model for shape memory materials. Part I. The monolithic shape memory alloy". *International Journal of Plasticity*, **12**(6), pp. 805–842.

[29] O'Handley, R. C., Allen, S. M., Paul, D. I., Henry, C. P., Marioni, M., Bono, D., Jenkins, C., Banful, A., and Wager, R., 2003. "Keynote address: Magnetic field-induced strain in single crystal Ni-Mn-Ga". *Proceedings of SPIE, Symposium on Smart Structures and Materials*, **5053**, pp. 200–206.

[30] Tickle, R., 2000. "Ferromagnetic shape memory materials". PhD thesis, University of Minnesota, May.